RNA (1998), *4*:719–728. Cambridge University Press. Printed in the USA.

Global structure of four-way RNA junctions studied using fluorescence resonance energy transfer

FRANK WALTER, ALASTAIR I.H. MURCHIE, DEREK R. DUCKETT,[1] and DAVID M.J. LILLEY

CRC Nucleic Acid Structure Research Group, Department of Biochemistry, The University of Dundee, Dundee DD1 4HN, United Kingdom

ABSTRACT

Four-way helical junctions are found widely in natural RNA species. In this study, we have studied the conformation of two junctions by fluorescence resonance energy transfer. We show that the junctions are folded by pairwise coaxial helical stacking, forming one predominant stacking conformer in both examples studied. At low magnesium ion concentrations, the helical axes of both junctions are approximately perpendicular. One junction undergoes a rotation into a distorted antiparallel structure induced by the binding of a single magnesium ion. By contrast, the axes of the four-way junction of the U1 snRNA remain approximately perpendicular under all conditions examined, and we have determined the stacking conformer adopted.

Keywords: branched RNA; FRET; metal ions; RNA structure; U1 snRNA

INTRODUCTION

The secondary structure of RNA molecules can be decomposed into a number of features, such as duplexes, loops, bulges, and hairpins [reviewed in Tinoco et al. (1990), Chastain & Tinoco (1991), and Lilley (1995)], and there have been a number of structural studies of representatives of all of these species [reviewed in Wyatt & Tinoco (1993)]. Helical junctions are further relatively common features of RNA secondary structure, with important consequences for the tertiary folding of RNA, yet, by contrast with other local structural elements, these have been much less studied. Nevertheless, helical branchpoints are common building elements in many functional RNA molecules. For example, mammalian and amphibian U1 snRNA contains a prominent four-way RNA junction [a 4H junction (Lilley et al., 1995)] that probably organizes the structure of the whole RNA molecule (Branlant et al., 1981). The natural form of the hairpin ribozyme in the negative strand satellite RNA of the tobacco ringspot virus is also a four-way junction (Hampel & Tritz, 1989), and it is thought that the two loop-containing arms that associate to form the active site for self-cleavage are adjacent arms of the perfect 4H junction. The sequences of the RNA of bacteriophages Qβ and MS2 indicate secondary structures that contain many potential three- (3H) and four-way junctions (Beekwilder et al., 1995; Groeneveld et al., 1995). Conformational transitions within these structures have been suggested to be important in the regulation of translation of the viral RNA (Poot et al., 1997).

We have previously studied the global conformation of a number of four-way RNA junctions, using comparative gel electrophoresis (Duckett et al., 1995). We found that all such junctions studied adopted a folded geometry based on pairwise coaxial stacking of helical arms, with a pronounced bias toward one stacking conformer for each junction (Fig. 1). Although this behavior is exhibited by DNA junctions (Duckett et al., 1988), the RNA junctions differed in two respects. First, the stacked structure was adopted under all conditions studied, including very low salt concentrations, where all DNA junctions are unstacked. Second, the RNA junctions tended to adopt a geometry where the two helical axes were at approximately 90°, in contrast to the invariant antiparallel cross of the DNA junction. On elevating divalent ion concentration, however, most RNA junctions rotated into a distorted antiparallel structure, although the U1 four-way junction remained in the 90° cross under all conditions.

One reason that the structures of helical junctions are less well characterized than other elementary features

Reprint requests to: David M.J. Lilley, CRC Nucleic Acid Structure Research Group, Department of Biochemistry, The University of Dundee, Dundee DD1 4HN, United Kingdom; e-mail: dmjlilley@bad.dundee.ac.uk.

[1]Present address: Department of Biochemistry, Box 3711, Duke University Medical Center, Durham, North Carolina 27710, USA.

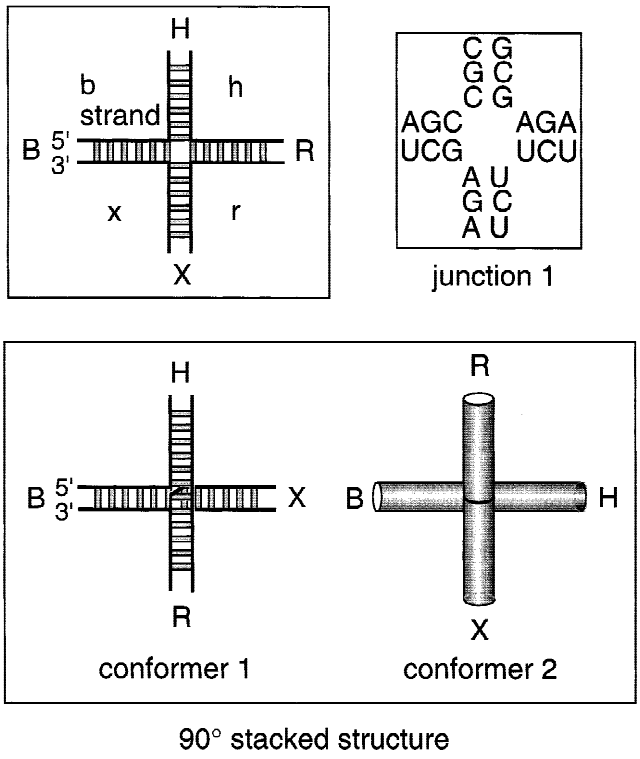

FIGURE 1. Four-way helical junctions in RNA. A four-way helical junction can be constructed from four separate oligonucleotides. In these studies, these are named b, h, r, and x, generating the four arms called B, H, R, and X, as shown. The central base sequence of junction 1 (Duckett et al., 1995) is shown. Comparative gel electrophoretic analysis has indicated that four-way RNA junctions undergo folding by pairwise coaxial stacking of arms, with a tendency to adopt the structure where the two resulting axes subtend an angle of 90°. There are two possible conformers of this structure, depending on the choice of stacking partners. It should be noted that, in the case of RNA junctions, we do not currently have any information on the handedness of structures, and this aspect is necessarily drawn arbitrarily.

in RNA is that their extended nature does not lend itself readily to conventional methods of structural analysis such as NMR, and techniques giving longer-range information are required. We have previously applied the methods of comparative gel electrophoresis to analyze the global structure of some four-way RNA junctions (Duckett et al., 1995); in the present study, we have applied another method well suited to the study of global structure, fluorescence resonance energy transfer (FRET). The efficiency of energy transfer between pairs of fluorophores attached to the 5′ termini of chosen pairs of helices is inversely proportional to the sixth power of the end-to-end distance in the range 20–80 Å, and the global geometry can thus be deduced by comparison of all the possible end-to-end vectors. This method has proved powerful in the study of four- (Murchie et al., 1989; Clegg et al., 1992, 1994) and three-way (Stühmeier et al., 1997) DNA junctions, bulged duplexes in DNA and RNA (Gohlke et al., 1994), the hammerhead ribozyme (Tuschl et al., 1994; Bassi et al., 1997), and the hairpin ribozyme (Murchie et al., 1998). In this paper, we have applied steady-state FRET measurements to analyze the global structure of the four-way RNA junction, and have confirmed and extended the conclusions from comparative gel electrophoresis.

RESULTS

Global conformational analysis of a four-way RNA junction

We selected junction 1 for initial study—a four-way junction that has been characterized extensively in DNA. It has been studied previously both in DNA and RNA form (Duckett et al., 1988, 1995). The central sequence is shown in Figure 1. We have previously used comparative gel electrophoresis to study the global conformation of an RNA junction based on the central sequence of junction 1 (Duckett et al., 1995). In this approach, we generate the six possible species with two long (40 bp) and two short (15 bp) arms derived from a four-way junction in which the central 10 bp of each arm are synthesized from ribonucleotides and the remainder is DNA. The four arms of the junctions are named sequentially B, H, R, and X, and the two-long, two-short arm species labeled according to the long arms. The electrophoretic mobility of the six species in a polyacrylamide gel are compared and analyzed on the assumption that the relative mobility reflects the angle subtended between the long arms.

We showed previously (Duckett et al., 1995) that we could obtain a pattern of electrophoretic mobilities in the absence of added magnesium ions that was consistent with a global structure derived by pairwise coaxial stacking of helical arms, where the two axes were mutually perpendicular. This is also the case in the presence of low concentrations of magnesium ions (Fig. 2a). The observed pattern is described by fast, slow, slow, slow, slow, fast, where the four slower species have equal mobility. The interpretation of this pattern is indicated beside the gel, based on the coaxial stacking of B on H and R on X arms, giving the four 90° (slow) species BR, BX, HR, and HX, and two 180° (faster) species BH and RX. This pattern of mobilities was also observed in the presence of 50 mM sodium or 20 μM hexammine cobalt (III) ions (data not shown). Upon increasing the concentration of magnesium ions, the pattern changes to one described by fast, intermediate, slow, slow, intermediate, fast (Fig. 2b), although this is significantly less symmetrical than that typically found for DNA junctions. We discuss the lowered symmetry below. But, to a first approximation, this pattern is consistent with a rotation of the stacked helical pairs in the direction of an antiparallel structure, as illustrated next to the autoradiograph in Figure 2b. A closely similar pattern of mobilities was found in the

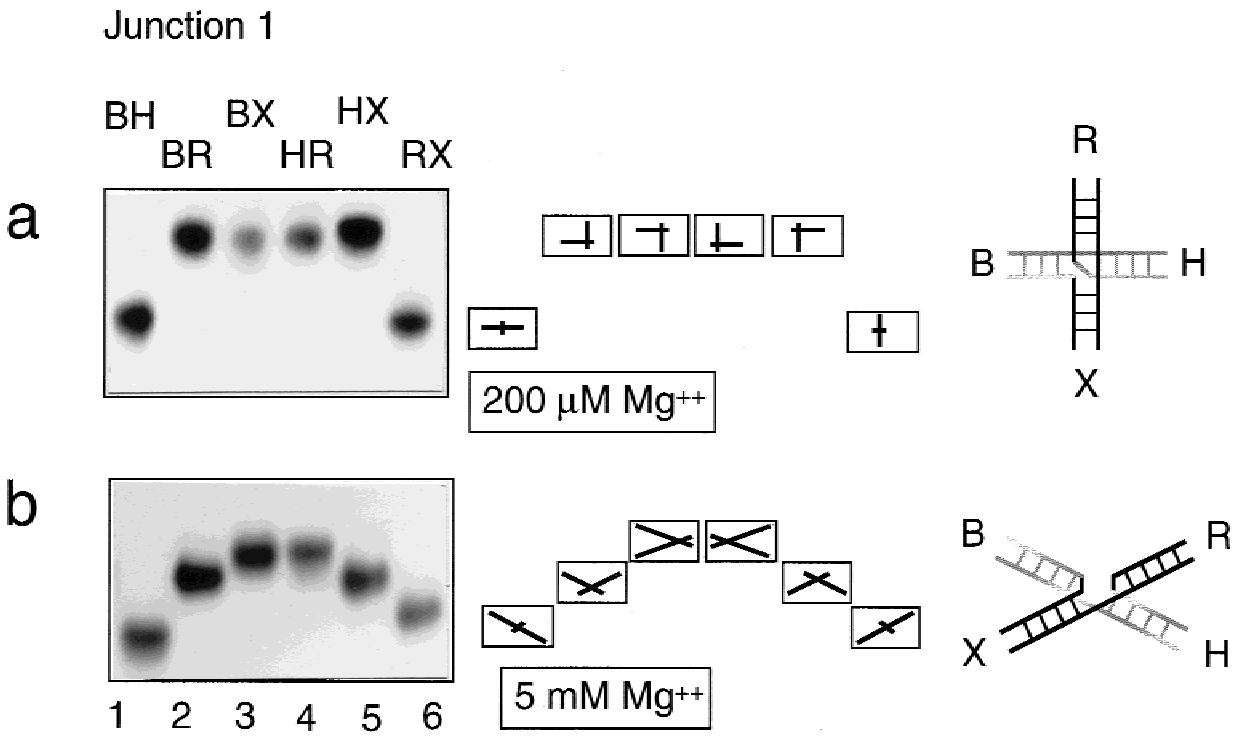

FIGURE 2. Global structure of junction 1 analyzed by comparative gel electrophoresis. For this analysis, the junction was generated from strands in which the central 20 nt was RNA and the remaining 30 nt at each end were DNA. The sequences of these strands ensured that they hybridized such that the point of strand exchange was located at the center. The six possible species having two long arms of 30 bp and two shorter arms of 10 bp were created and named according to the long arms (e.g., species BH has long B and H arms, and short R and X arms). The six long–short species were electrophoresed in a polyacrylamide gel in the presence of 90 mM Tris·borate (pH 8.3) with the indicated magnesium ion concentration. Because the junctions were created from strands that were radioactively [5′-^{32}P] labeled, the RNA species were revealed by autoradiography of dried gels. **a:** Analysis in the presence of 200 μM magnesium ions. The six long–short species migrate in a pattern interpreted in terms of a 90° stacked structure based on B on H stacking, indicated far right. This generates the predicted long–short species shown right. **b:** Analysis in the presence of 5 mM magnesium ions. Under these conditions, the six long–short species give a pattern that is consistent with the antiparallel structure, indicated far right, to a first approximation. This generates the predicted long–short species shown center. Tracks in (a) and (b): track 1, BH species; track 2, BR species; track 3, BX species; track 4, HR species; track 5, HX species; track 6, RX species.

presence of a lower concentration of calcium ions (Duckett et al., 1988).

In summary, the comparative gel electrophoretic analysis indicates that the four-way DNA junction 1 adopts a coaxially stacked structure based on B on H stacking, with an angle between axes dependent on divalent ion concentration. Under many conditions, the angle subtended between axes is close to 90°, whereas, in the presence of higher magnesium ion concentrations, the structure becomes antiparallel.

FRET analysis of global structure

FRET provides an alternative method for the study of global conformation of branched nucleic acid in solution. In this method, we compare the relative end-to-end distances for selected pairs of helical arms by studying the efficiency of resonance energy transfer (E_{FRET}) between donor and acceptor fluorophores covalently attached to the termini of pairs of arms. E_{FRET} is related to the distance between the fluorophores (R) by (Förster, 1948):

$$E_{FRET} = \{1 + (R/R_0)^6\}^{-1}, \quad (1)$$

where R_0 is a length characteristic of the fluorophores used that is related to the distance at which E_{FRET} is half-maximal. Provided that the junction comprises four arms of equal length, comparison of the six end-to-end distances gives an indication of the global structure of the junction, and this may be studied as a function of ionic conditions.

FRET analysis of the global structure of junction 1

Junctions based on the sequence of junction 1 were constructed from four 20-nt ribooligonucleotides, where the 5′-terminal nucleotide was substituted by a deoxyribonucleotide. The point of strand exchange was cen-

trally located, giving four arms, each of 10 bp in length. Donor and acceptor fluorophores were attached to the 5′ ends of individual strands, thus placing them at the ends of chosen arms in a pairwise manner (Fig. 3). There are six end-to-end vectors that can be studied in this manner, each of which can be labeled in both directions. In order to keep the environment for the fluorophores constant, the 5′ sequence of each component strand was 5′CC; we found previously that 5′CC sequences are well-behaved in fluorescence experiments. The fluorophores used in these studies were fluorescein (donor) and cyanine-3 (Cy-3, acceptor). In order to gauge the mobilities of the fluorophores attached to the junctions, we measured the anisotropy values (r). Although the Cy-3 was relatively constrained ($r = 0.33$), the fluorescein was mobile ($r = 0.15$), and thus we may interpret the E_{FRET} values in terms of relative distances. All spectra were recorded at 5 °C, a temperature that is >20° below the melting temperature for these junctions under all conditions (data not shown).

Fluorescence spectra were recorded under two sets of conditions. The first entailed excitation at 490 nm, where fluorescein is principally, but not exclusively, excited. The acceptor component was derived by subtraction of a pure fluorescein spectrum. The second spectrum was acquired by excitation at 547 nm, where Cy-3 is exclusively excited. The normalized acceptor emission was derived by taking the ratio [called $(ratio)_A$ (Clegg, 1992)] of these two spectra, which is directly related to E_{FRET}.

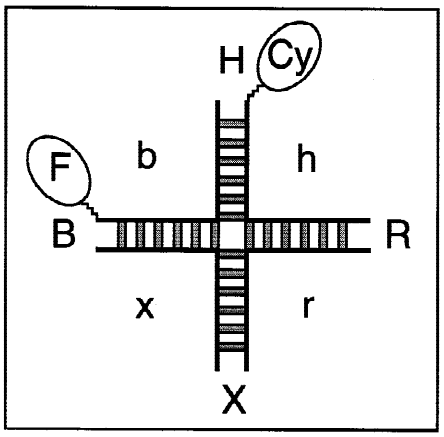

FIGURE 3. Fluorescently labeled junctions used in FRET analysis of global conformation. Junctions for FRET studies were constructed from four RNA oligonucleotides each of 20 nt, giving four arms each of 10 bp in length. One strand carries fluorescein attached to the 5′ end, a second strand carries Cy-3 attached to its 5′ end, and the remaining two are unlabeled. There are six possible end-to-end vectors that can be compared, each of which can be labeled in two directions. The species are named by the arms that carry the fluorophores, in the order donor–acceptor. The example shown is vector BH, carrying fluorescein on the B arm and Cy-3 on the H arm. The reversed vector would be HB, with fluorescein on the H arm and Cy-3 on the B arm.

Figure 4a shows a plot of the E_{FRET} values for the six possible end-to-end distances in the absence of added magnesium ions. Most of the vectors give values around 0.3 or less, indicative of a relatively extended structure. Two of the vectors exhibit lower values of E_{FRET} (0.2), indicating that the HB and XR end-to-end distances are longer than the remaining four. This is consistent with a 90° crossed stacked structure based on B on H stacking, such that the longer end-to-end distances are the diagonals formed by the coaxially stacked helices, i.e., HB and XR.

Upon addition of magnesium ions (Fig. 4b,c), there is a change in the relative E_{FRET} values, where the efficiencies for the XB and RH vectors become significantly greater than the remaining four end-to-end vectors, at the expense of the RB and XH vectors, where E_{FRET} is reduced to 0.2. This is the pattern of efficiencies expected if the structure is rotated toward the antiparallel structure, where the XB and RH end-to-end distances are the shortest.

The pattern of efficiencies is not completely symmetrical in the presence of magnesium ions. For example, in 10 mM magnesium ions, it is clear that E_{FRET} for RH is greater than that for XB. This difference is significant. We repeated the measurements under the same conditions (10 mM magnesium ions) for a second set of species where the fluorophores were reversed. Comparison of Figure 4c and d shows that the patterns of E_{FRET} values are closely similar, including the disparity between the values for the BX and HR vectors, despite the reversal of labeling and the complete de novo synthesis and construction of new species. We conclude that the HR end-to-end distance is significantly shorter than that for BX, consistent, for example, with a break in the axis of the R-X arms. This distortion from a perfect stacked X-structure would explain the asymmetry in the pattern of electrophoretic mobilities, tending to retard the mobility of the RX species relative to the BH species, as observed (Fig. 2).

Magnesium ion binding and the folding of junction 1

Junction 1 undergoes a change in global conformation induced by the addition of magnesium ions. This suggests a conformational equilibrium of the type:

$$J_{90} + n\mathrm{Mg}^{2+} \leftrightarrow J_{AP}\cdot(\mathrm{Mg}^{2+})_n,$$

where J_{90} is the junction in the 90° crossed conformation and J_{AP} is that in the antiparallel conformation. The proportion of junction in the antiparallel form (α) will be given by:

$$\alpha = K_A\cdot[\mathrm{Mg}^{2+}]^n/(1 + K_A\cdot[\mathrm{Mg}^{2+}]^n), \qquad (2)$$

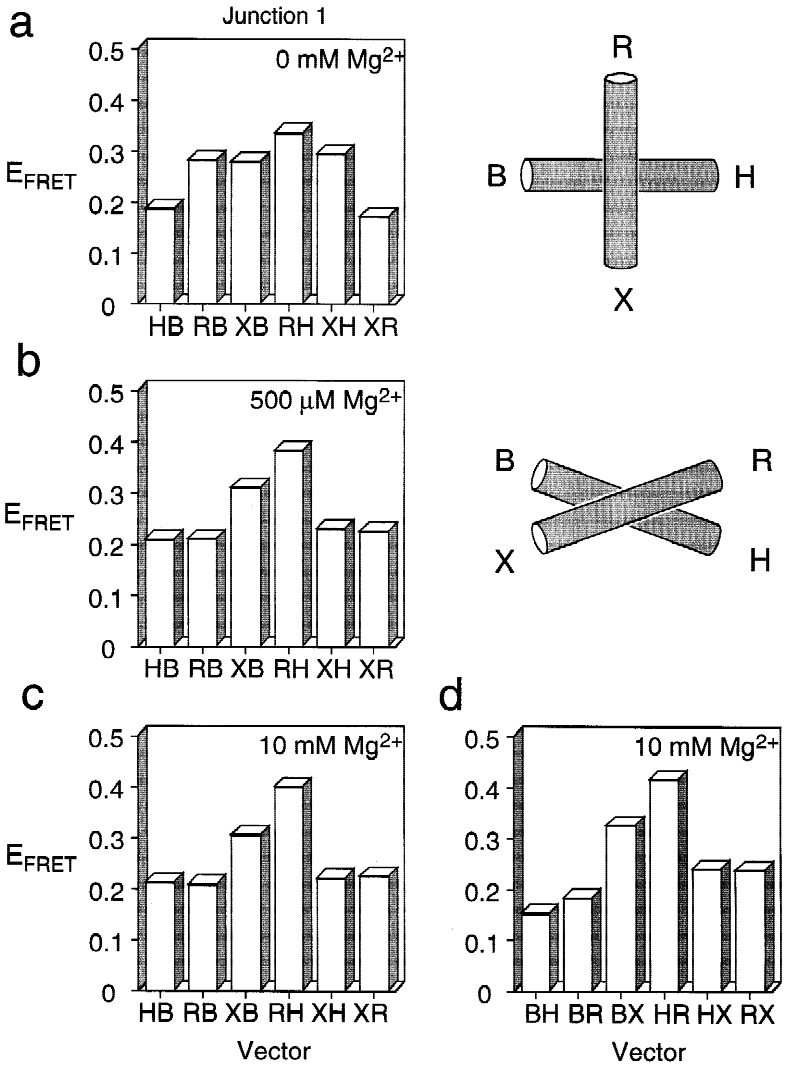

FIGURE 4. Global structure of junction 1 analyzed by FRET. The efficiency of energy transfer was measured for each end-to-end vector. **a:** Plot of E_{FRET} values for one series of six end-to-end vectors in the absence of magnesium ions. Under these conditions, the vectors HB and XR exhibit slighly lower values of E_{FRET} compared to the remaining four end-to-end vectors, consistent with the 90° stacked structure based on B on H stacking (indicated right). **b:** Plot of E_{FRET} values for the six end-to-end vectors labeled as in (a) in the presence of 500 μM magnesium ions. Comparison with (a) shows that the efficiency for the end-to-end vectors XB and RH has risen, consistent with a rotation in the antiparallel direction (indicated right). However, the structure appears to be less symmetrical than the simple stacked X-structure illustrated, such that the distances RH $<$ XB. **c:** Plot of E_{FRET} values for the six end-to-end vectors labeled as in (a) in the presence of 10 mM magnesium ions. This pattern of efficiencies is essentially the same as that found (b) in the presence of 500 μM magnesium ions. **d:** Plot of E_{FRET} values in the presence of 10 mM magnesium ions for the six end-to-end vectors labeled in the opposite direction to that in (c). The relative efficiencies for the six end-to-end vectors is closely similar to that for the reverse vectors, showing that the results are not dependent on the direction of labeling.

where K_A is the apparent association constant for magnesium ions. E_{FRET} for the HR vector was remeasured over a finer range of magnesium ion concentrations, and the data are plotted in Figure 5. The data were fitted using the model represented by Equation 1. A good fit (correlation coefficient of 0.995) to the experimental E_{FRET} values was obtained, giving a value of $n = 0.999$. We conclude that the binding of a single magnesium ion is responsible for inducing the change in conformation that we observe by the fluorescence measurements. The calculated association constant is $7.2 \pm 1.1 \times 10^3$ M^{-1}.

Global structure of the U1 four-way junction

The mammalian and amphibian U1 snRNA provides a good natural example of a four-way junction in a functional RNA molecule. The sequence of the junction (Fig. 6) is widely conserved (Branlant et al., 1981). It is a perfect four-way junction apart from the G·A mismatch in one arm at the point of strand exchange. Previous comparative gel electrophoretic analysis has indicated that the junction is folded by pairwise coaxial stacking of arms as shown in the figure, such that the A of the G·A mismatch is located on the continuous strand (the A_c conformer). However, in contrast to junction 1, it was found that the U1 junction remained in the 90° crossed conformation both in the absence of magnesium ions and in the presence of 1 mM magnesium ions. This appears to be general for all conditions examined. Figure 7 shows results of comparative gel electrophoretic analysis of the human U1 junction in the presence of 100 μM magnesium ions. The pattern is clearly described by slow, slow, fast, fast, slow, slow, indicating a 90° crossed structure based on the stacking of B (arm containing G·A mismatch) on X (arm containing bulged C) arms, i.e., the A_c conformer. There is a slight distortion of the perfect 90° pattern in favor of one with a small rotation toward the antiparallel structure, indicated by the slightly faster mobility of the BR

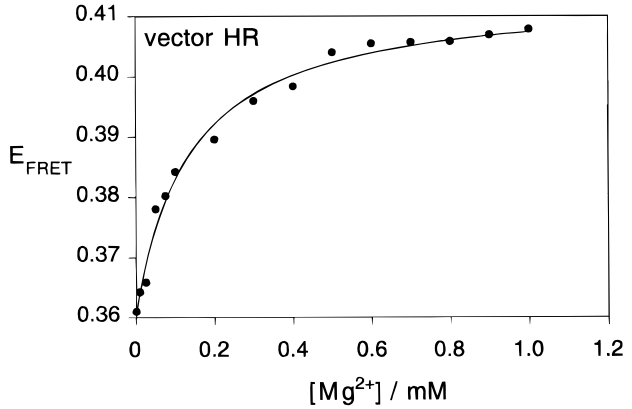

FIGURE 5. Magnesium ion-induced folding of junction 1. Folding of junction 1 was followed over a finer range of magnesium ion concentration by studying the efficiency of energy transfer for the end-to-end vector HR. Measured E_{FRET} values are plotted as a function of magnesium ion concentration (data points). These data were fitted by a two-state model in which the binding of n magnesium ions induces the change in end-to-end length (see text). The fit generated (line) gives a value for $n = 0.999$, i.e., indicates that the transition to the antiparallel structure is induced by the binding of a single magnesium ion.

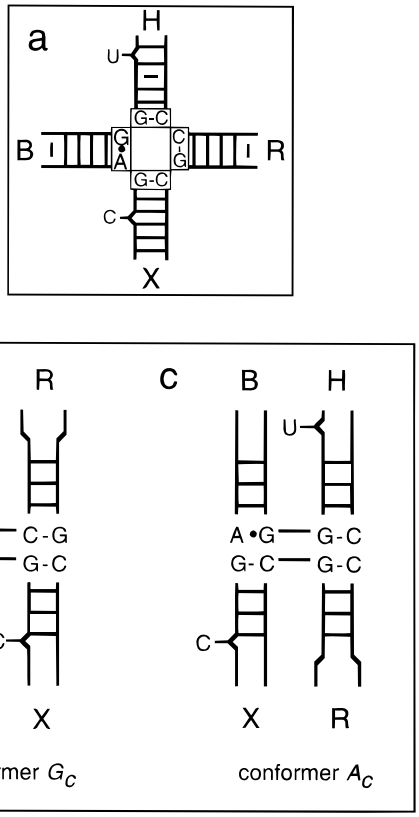

FIGURE 6. Four-way junction of the U1 snRNA. **a:** Schematic to show the secondary structure of the four-way junction of human U1 RNA (Branlant et al., 1981). The four central base pairs are shown, including the terminal G·A mispair of the B arm. The positions of bulged bases and mispairs (short bars) are indicated. For the purpose of the analysis of global conformation, we have labeled the four arms B, H, R, and X as shown. There are two potential stacking conformers of this structure. In the constructs used here, all mismatches (other than the central G·A) and bulges were removed, because local kinks could add vectorially to that at the junction and thus complicate the analysis of the global structure of the junction itself. **b,c:** Conformer G_c (b) is formed by the coaxial stacking of H on B arms, and places the guanine base of the G·A mispair on the continuous strand. Conformer A_c (c) is formed by the coaxial stacking of B on X arms, and places the adenine base of the G·A mispair on the continuous strand.

and HX species compared to the BH and RX species. The structure does not appear to depend detectably on the presence of the A·G mismatch (Duckett et al., 1995).

Analysis of the conformation of the U1 junction by FRET

Fluorophore-labeled junctions based on the sequence of the human U1 junction were constructed analogously to those for the FRET analysis of junction 1. Junctions with four arms each of 10 bp were assembled from four 20-nt ribooligonucleotides, where the 5′-terminal nucleotide was substituted by a deoxyribonucleotide. Each junction was constructed from two unlabeled strands, one 5′ labeled with fluorescein and one 5′ labeled with Cy-3. As before, the 5′ sequence of each component strand was 5′ CC.

The efficiencies of energy transfer for the six end-to-end vectors of the U1 junctions are shown in Figure 8. A similar pattern of E_{FRET} values is found under all conditions from 0 to 10 mM magnesium ions, where the efficiencies of the BX and HR vectors ($E_{FRET} \approx 0.2$) are lower than the remaining four vectors, showing that the B to X and H to R distances are longer than the others. This is consistent with an approximately 90° crossed structure based on B on X stacking, where B-X and H-R are the diagonals of the square. The FRET results are thus in full agreement with those of the comparative gel electrophoresis.

DISCUSSION

The formation of a coaxially stacked structure in one predominant stacking conformer is supported by both comparative gel electrophoresis and FRET, both for junction 1 and the naturally occurring junction of the U1 snRNA. The stacked conformation is stable even at low ionic strength, conditions under which four-way DNA junctions are unstacked (Duckett et al., 1988). However, we have not found any conditions under which four-way RNA junctions are opened into a structure lacking coaxial helical stacking. The stacked–unstacked equilibrium reflects the balance between the electrostatic repulsion tending to open the junction into an extended structure, and the short-range forces that stabilize a coaxially stacked structure. In the case of the RNA junction, this balance is clearly biased toward the stacked structure under all conditions examined, indicating that the free energy of forming a stacked structure outweighs electrostatic repulsion in the unscreened

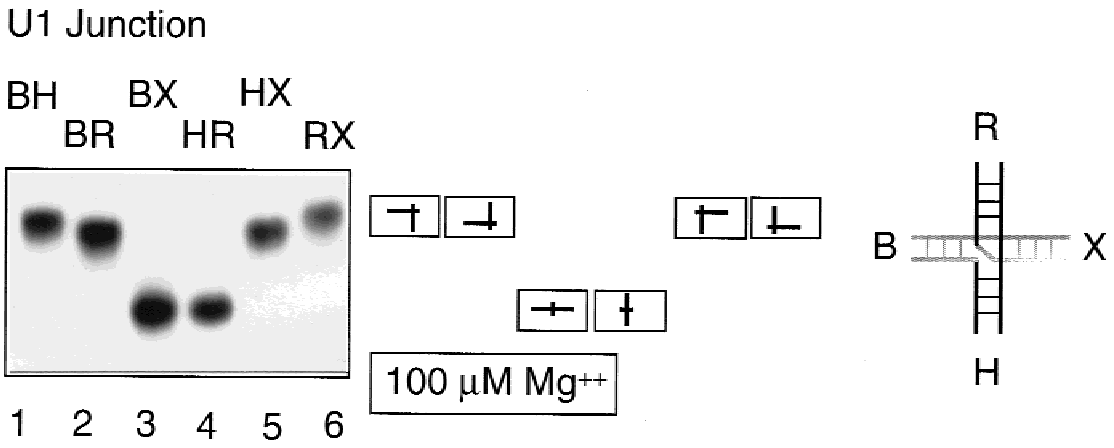

FIGURE 7. Global structure of the U1 junction analyzed by comparative gel electrophoresis in the presence of 100 μM magnesium ions. The six long–short species derived from a four-way junction having an RNA core with the sequence of the U1 junction (Duckett et al., 1995) were electrophoresed in a polyacrylamide gel in the presence of 90 mM Tris·borate (pH 8.3), 100 μM $MgCl_2$. The radioactive RNA junction species were revealed by autoradiography of the dried gel. The slow, slow, fast, fast, slow, slow pattern of mobilities obtained indicates that the U1 junction adopts a 90° crossed structure based on B on X stacking (indicated right) under these conditions. Track 1, BH species; track 2, BR species; track 3, BX species; track 4, HR species; track 5, HX species; track 6, RX species.

structure for the RNA junctions. This could result from either a greater stability of the stacked structure, or a lowered electrostatic repulsion in the RNA structure.

Junction 1 is folded by the coaxial stacking of B on H, and X on R arms. This is demonstrated by the relatively long B-H and R-X distances indicated by the FRET measurements, and by the faster mobility of the BH and RX species in the comparative gel electrophoresis experiments. The two pairs of stacked arms subtend angles of approximately 90° under conditions of low divalent cation concentrations, including in the presence of relatively high sodium ion concentrations. Upon addition of magnesium [or calcium (Duckett et al., 1995)] ions, the junction undergoes a change of conformation that involves a rotation of the helices to form an antiparallel structure, resulting in a shortening (increased E_{FRET}) of the B-X and H-R distances. This conformational change is induced by the binding of a single magnesium ion, with an apparent association constant in the region of 7,000 M^{-1}. Both the FRET and the comparative gel electrophoresis experiments indicate a significant asymmetry in the antiparallel stacked structure, however, consistent with a disruption of coaxial character for the R-X helices. This might be a consequence of the helical geometry of double-stranded RNA. Although the structure of B-DNA lends itself to a favorable juxtaposition of backbones and major grooves in the antiparallel stacked X-structure (Murchie et al., 1989; von Kitzing et al., 1990), this is harder if not impossible to achieve for an A-form helix. Perhaps the antiparallel structure cannot be formed without some distortion of one of the stacked helical pairs.

In contrast to junction 1, the junction of the U1 snRNA appears to be fixed in the near-90° crossed conformation, and the conformation is insensitive to the presence or absence of divalent cations. This is supported by both comparative gel electrophoresis and FRET analysis. This may indicate that some aspect of the sequence of this junction is preventing the transition into the antiparallel structure, although some comparative gel electrophoretic studies indicate a degree of antiparallel structure. The lower E_{FRET} values for the B-X and H-R distances show that the predominant stacking conformer is that based on B on X and H on R stacking, in agreement with the comparative gel electrophoresis. This structure has been termed the A_c conformer, because it places the A of the A·G mismatch on the continuous strand. The relative stability of this conformer is in full agreement with an early prediction based on molecular modeling in conjunction with chemical modification data (Krol et al., 1990). Despite the presence of a base mismatch at the point of strand exchange, it does not appear to play a crucial role in determining conformer bias. The choice of stacking partner remains unaltered if the A·G mismatch is changed to either of the Watson–Crick pairs AU or CG (Duckett et al., 1995). The sequence, including the mismatch, is well conserved in mammalian and amphibian U1 RNA (Branlant et al., 1981), but, in *Drosophila*, the corresponding base pair is an AU pair. Yet, comparative gel electrophoresis experiments showed that an RNA junction based on the *Drosophila* U1 snRNA sequence adopted the equivalent stacking conformer (Duckett et al., 1995), and thus the tertiary structure of this RNA appears to be highly conserved.

This study demonstrates the close qualitative agreement between FRET and comparative gel electrophoresis. Both methods agree on the global structures

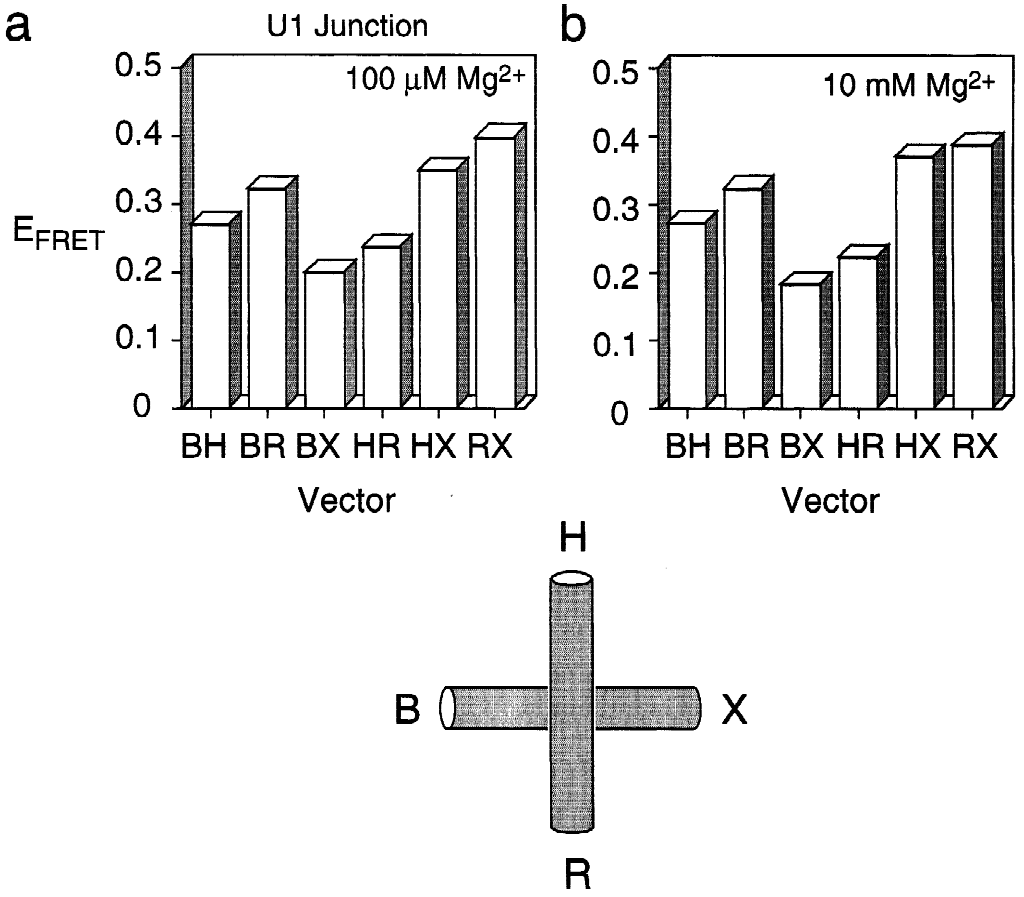

FIGURE 8. Global structure of the U1 junction analyzed by FRET. The six doubly terminally labeled species of junction 1 were prepared using fluorescein and Cy-3. The efficiency of energy transfer was measured for each end-to-end vector using the $(ratio)_A$ method of acceptor normalization (Murchie et al., 1989; Clegg, 1992) and plotted for each vector. **a:** Plot of E_{FRET} values for the six end-to-end vectors in the presence of 100 μM magnesium ions. Under these conditions, the vectors BX and HR exhibit slighly lower values of E_{FRET} compared to the remaining four end-to-end vectors, consistent with the 90° stacked structure based on B on X stacking (i.e., the A_c conformer). **b:** Plot of E_{FRET} values for the six end-to-end vectors in the presence of 10 mM magnesium ions. The pattern of E_{FRET} values are closely similar to those at lower magnesium ion concentrations [compare with (a)], indicating that the 90° stacked A_c conformer exists under all conditions.

adopted by the junctions examined, including the choice of stacking partners. This provides confidence in each method for the analysis of global structure in branched RNA species. On a quantitative level, there are some discrepancies. The transition of junction 1 into the antiparallel structure was well advanced at a magnesium concentration of 200 μM, whereas, under the conditions of the gel electrophoresis, the structure remained essentially that of the 90° cross. This probably reflects differences between the environment of the gel pores and that of the bulk solution.

The nature of the four-way junction is such that it is likely to play a central role in organizing the tertiary structure of RNA molecules that contain it. It is rather probable that the overall structure of the U1 snRNA will be heavily influenced by the conformation of the junction, for example, and there is evidence that conformational transitions in junctions in MS2 RNA control translation of the maturation gene (Poot et al., 1997). Understanding the structures, thermodynamics, and kinetic features of these structures is therefore important.

MATERIALS AND METHODS

DNA, RNA, and mixed DNA–RNA oligonucleotides were synthesized using phosphoramidite chemistry (Beaucage & Caruthers, 1981) implemented on Applied Biosystems 394 synthesizers. Fluorescently labeled species were prepared as described in Bassi et al. (1997). RNA was synthesized using ribonucleotide phosphoramidites with 2′-*tert* butyldimethylsilyl (TBDMS) protection (Hakimelahi et al., 1981; Perreault et al., 1990) (Glen Research). 6-Fluorescein (PE-ABI) and sulphoindocarbocyanine (Cy-3; Glen Research) were coupled to the 5′-termini as phosphoramidites. Oligoribonucleotides were deprotected in 25% ethanol/ammonia solution at 55 °C for 6 h (dye labeled) or 12 h (unlabeled) and evaporated to dryness. Oligoribonucleotides were redissolved in 0.5 mL 1 M tetrabutylammonium fluoride (TBAF; Aldrich) in tetrahydrofuran to remove TBDMS groups and agitated at

20 °C in the dark for 16 h prior to desalting by G25 Sephadex (NAP columns; Pharmacia) and ethanol precipitation. Fully deprotected oligonucleotides were purified by gel electrophoresis in 20% polyacrylamide containing 7 M urea; fluorescently labeled species were significantly retarded in the gel system. Bands were excised, and the oligonucleotides electroeluted into 8 M ammonium acetate and recovered by ethanol precipitation. Fluorescently labeled oligonucleotides were further purified by reversed-phase HPLC. Samples were dissolved in 100 mM ammonium acetate and applied to a C18 reversed-phase column (μ Bondapak, Waters). RNA was eluted with a linear gradient of acetonitrile; buffer A: 100 mM ammonium accetate, buffer B: acetonitrile, with a flow rate of 1 mL/min. The peak fractions were evaporated to dryness, redissolved in water, and then ethanol precipitated. Absorption spectra of fluorescently labeled RNA were recorded on a Cary 1E spectrometer.

Each fluorescent junction species for FRET studies was constructed from two unlabeled strands, one strand labeled with fluorescein and one Cy-3-labeled strand, placing the fluorophores at the ends of a given pair of arms. The junctions were hybridized by incubating stoichiometric amounts of the four appropriate RNA oligonucleotides in 90 mM Tris-borate, pH 8.3, 25 mM NaCl for 10 min at 80 °C, followed by slow cooling. The hybridized junctions were loaded onto an 8% polyacrylamide gel and electrophoresed at 4 °C for 22 h at 150 V. The buffer system contained 90 mM Tris-borate, pH 8.3, 25 mM NaCl, and was recirculated at $>$ 1 L/h. Fluorescent junctions were visualized by direct exposure to a standard lamp, the bands were excised, and the RNA was electroeluted into 8 M ammonium acetate and recovered by ethanol precipitation.

Comparative gel electrophoresis

Electrophoresis was performed as described in Duckett et al. (1995). Sixteen DNA/RNA oligonucleotides were synthesized for each junction, of which the four longest ones had the sequences (all written 5′ to 3′, with DNA sections underlined):

Junction 1

b strand: CGCAAGCGACAGGAACCTCGAGGGATCCGTCCUAGCAAGCCGCUGCUACCGGAAGCTTCTCGAGGTTCCTGTCGCTTGCG

h strand: CGCAAGCGACAGGAACCTCGAGAAGCTTCCGGUAGCAGCGAGAGCGGUGGTTGAATTCCTCGAGGTTCCTGTCGCTTGCG

r strand: CGCAAGCGACAGGAACCTCGAGGAATTCAACCACCGCUCUUCUCAACUGCAGTCTAGACTCGAGGTTCCTGTCGCTTGCG

x strand: CGCAAGCGACAGGAACCTCGAGTCTAGACTGCAGUUGAGAGCUUGCUAGGACGGATCCCTCGAGGTTCCTGTCGCTTGCG

Human U1 junction

b strand: CGCAAGCGACAGGAACCTCGAGGGATCCGTCCUAGGCAGGGGAGAUACGCGGAAGCTTCTCGAGGTTCCTGTCGCTTGCG

h strand: CGCAAGCGACAGGAACCTCGAGAAGCTTCCGGGUAUCUCCCAGGGCGUGGTTGAATTCCTCGAGGTTCCTGTCGCTTGCG

r strand: CGCAAGCGACAGGAACCTCGAGGAATTCAACCACGCCCUGCGAGUUUUGCAGTCTAGACTCGAGGTTCCTGTCGCTTGCG

x strand: CGCAAGCGACAGGAACCTCGAGTCTAGACTGCAAAACUCGACUGCCUAGGACGGATCCCTCGAGGTTCCTGTCGCTTGCG

The sequences of the remaining 12 oligonucleotides for each junction can be derived by deletion of 25 nt at the 5′, 3′, or both termini.

Fluorescence spectroscopy

Spectra were recorded at 5 °C in 90 mM Tris·borate, pH 8.3, with the indicated concentrations of magnesium ions. Fluorescence spectroscopy was performed on an SLM-Aminco 8100 fluorimeter operating in photon-counting mode, and spectra were corrected for lamp fluctuations and instrumental variations, as described in Bassi et al. (1997). Spectra were recorded with excitation and emission polarizers set at 54.74° to avoid polarization artifacts. FRET efficiencies were measured using the $(ratio)_A$ method (Murchie et al., 1989; Clegg, 1992). An extracted acceptor spectrum $F^A(\nu_1,\nu')$ (excitation at $\nu' = 490$ nm, with emission at ν_1) is normalized to a further spectrum ($F(\nu_2,\nu'')$) excited at a wavelength ($\nu'' = 547$ nm) at which only the acceptor absorbs, with emission at ν_2. The acceptor ratio is calculated:

$$(ratio)_A = F^A(\nu_1,\nu')/F(\nu_2,\nu'')$$
$$= \{E_{\mathrm{FRET}}\cdot d^+\cdot(\epsilon^D(\nu')/\epsilon^A(\nu'')) + (\epsilon^A(\nu')/\epsilon^A(\nu''))\}$$
$$\cdot(\Phi^A(\nu_1)/\Phi^A(\nu_2)). \quad (3)$$

Superscripts D and A refer to donor and acceptor, respectively. ϵ^D and ϵ^A are the molar absorption coefficients at the indicated frequency of donor and acceptor, respectively, and Φ^A is the fluorescent quantum yield of the acceptor. E_{FRET} can be readily calculated because $\epsilon^D(\nu')/\epsilon^A(\nu'')$ and $\epsilon^A(\nu')/\epsilon^A(\nu'')$ are measured from absorption spectra, and $\Phi^A(\nu_1)/\Phi^A(\nu_2)$ is unity when $\nu_1 = \nu_2$. Fluorescence anisotropy values (r) were determined from measurements of fluorescence intensity using vertical excitation and emission polarizers ($F_\parallel$), and vertical excitation and horizontal emission polarizers ($F_\perp$, corrected for polarization artifacts). Fluorescence anisotropy was calculated from:

$$r = (F_\parallel - F_\perp)/(F_\parallel + 2\cdot F_\perp). \quad (4)$$

FRET experiments were performed on junctions derived from oligonucleotides of the following sequences:

Junction 1
b strand CCUAGCAAGCCGCUGCUAGG
h strand CCUAGCAGCGAGAGCGGUGG

r strand CCACCGCUCUUCUCAACUGG
x strand CCAGUUGAGAGCUUGCUAGG

Human U1 junction
b strand CCUAGGCAGGGGAGAUACGG
h strand CCGUAUCUCCCAGGGCGUGG
r strand CCACGCCCUGCGAGUUUUGG
x strand CCAAAACUCGACUGCCUAGG

ACKNOWLEDGMENTS

We are grateful to Drs. R. Clegg and G. Bassi for valuable discussion, and the CRC and BBSRC for financial support.

Received February 20, 1998; returned for revision March 10, 1998; revised manuscript received March 18, 1998

REFERENCES

Bassi GS, Murchie AIH, Walter F, Clegg RM, Lilley DMJ. 1997. Ion-induced folding of the hammerhead ribozyme: A fluorescence resonance energy transfer study. *EMBO J 16*:7481–7489.

Beaucage SL, Caruthers MH. 1981. Deoxynucleoside phosphoramidites—A new class of key intermediates for deoxypolynucleotide synthesis. *Tetrahedron Lett 22*:1859–1862.

Beekwilder MJ, Nieuwenhuizen R, van Duin J. 1995. Secondary structure model for the last two domains of single-stranded RNA phage Qβ. *J Mol Biol 247*:903–917.

Branlant C, Krol A, Ebel JP. 1981. The conformation of chicken, rat and human U1A RNAs in solution. *Nucleic Acids Res 9*:841–858.

Chastain M, Tinoco JI. 1991. Structural elements in RNA. *Prog Nucleic Acid Res Mol Biol 41*:131–177.

Clegg RM. 1992. Fluorescence resonance energy transfer and nucleic acids. *Methods Enzymol 211*:353–388.

Clegg RM, Murchie AIH, Zechel A, Carlberg C, Diekmann S, Lilley DMJ. 1992. Fluorescence resonance energy transfer analysis of the structure of the four-way DNA junction. *Biochemistry 31*:4846–4856.

Clegg RM, Murchie AIH, Zechel A, Lilley DMJ. 1994. The solution structure of the four-way DNA junction at low salt concentration; a fluorescence resonance energy transfer analysis. *Biophys J 66*:99–109.

Duckett DR, Murchie AIH, Diekmann S, von Kitzing E, Kemper B, Lilley DMJ. 1988. The structure of the Holliday junction and its resolution. *Cell 55*:79–89.

Duckett DR, Murchie AIH, Lilley DMJ. 1995. The global folding of four-way helical junctions in RNA, including that in U1 snRNA. *Cell 83*:1027–1036.

Förster T. 1948. Zwischenmolekulare Energiewanderung und Fluoreszenz. *Ann Phys 2*:55–75.

Gohlke C, Murchie AIH, Lilley DMJ, Clegg RM. 1994. The kinking of DNA and RNA helices by bulged nucleotides observed by fluorescence resonance energy transfer. *Proc Natl Acad Sci USA 91*:11660–11664.

Groeneveld H, Thimon K, van Duin J. 1995. Translational control of maturation-protein synthesis in phage MS2. A role for the kinetics of RNA folding? *RNA 1*:79–88.

Hakimelahi GH, Proba ZA, Ogilvie KK. 1981. High yield selective 3′-silylation of ribonucleosides. *Tetrahedron Lett 22*:5243–5246.

Hampel A, Tritz R. 1989. RNA catalytic properties of the minimum (−)sTRSV sequence. *Biochemistry 28*:4929–4933.

Krol A, Westhof E, Bach M, Lührmann R, Ebel JP, Carbon P. 1990. Solution structure of human U1 snRNA. Derivation of a possible three-dimensional model. *Nucleic Acids Res 18*:3803–3811.

Lilley DMJ. 1995. RNA structure and interactions with proteins. In: Lamond AI, ed. *Pre-mRNA processing*. Austin, TX: R.G. Landes. pp 1–15.

Lilley DMJ, Clegg RM, Diekmann S, Seeman NC, von Kitzing E, Hagerman P. 1995. Nomenclature committee of the International Union of Biochemistry: A nomenclature of junctions and branchpoints in nucleic acids. Recommendations 1994. *Eur J Biochem 230*:1–2.

Murchie AIH, Clegg RM, von Kitzing E, Duckett DR, Diekmann S, Lilley DMJ. 1989. Fluorescence energy transfer shows that the four-way DNA junction is a right-handed cross of antiparallel molecules. *Nature 341*:763–766.

Murchie AIH, Thomson JB, Walter F, Lilley DMJ. 1998. Folding of the hairpin ribozyme in its natural conformation achieves close physical proximity of the loops. *Molecular Cell.* in press.

Perreault JP, Wu T, Cousineau B, Ogilvie KK, Cedergren R. 1990. Mixed deoxyribo- and ribooligonucleotides with catalytic activity. *Nature 344*:565–567.

Poot RA, Tsareva NV, Boni IV, van Duin J. 1997. RNA folding kinetics regulates translation of phage MS2 maturation gene. *Proc Natl Acad Sci USA 94*:10110–10115.

Stühmeier F, Welch JB, Murchie AIH, Lilley DMJ, Clegg RM. 1997. The global structure of three-way DNA junctions with and without bulges: Fluorescence studies. *Biochemistry 36*:13530–13538.

Tinoco I, Puglisi JD, Wyatt JR. 1990. RNA folding. In: Eckstein F, Lilley DMJ, eds. *Nucleic acids & molecular biology, vol 4*. Berlin/Heidelberg: Springer-Verlag. pp 205–226.

Tuschl T, Gohlke C, Jovin TM, Westhof E, Eckstein F. 1994. A three-dimensional model for the hammerhead ribozyme based on fluorescence measurements. *Science 266*:785–789.

von Kitzing E, Lilley DMJ, Diekmann S. 1990. The stereochemistry of a four-way DNA junction: A theoretical study. *Nucleic Acids Res 18*:2671–2683.

Wyatt JR, Tinoco I. 1993. RNA structural elements and RNA function. In: Gesteland RF, Atkins JF, eds. *The RNA world*. Cold Spring Harbor, New York: Cold Spring Harbor Laboratory Press. pp 1–630.